Solution Structure of *N*-(2-Deoxy-D-*erythro*-pentofuranosyl)urea Frameshifts, One Intrahelical and the Other Extrahelical, by Nuclear Magnetic Resonance and Molecular Dynamics†

Virginie Gervais,‡ Jean A. H. Cognet,§ André Guy,|| Jean Cadet,|| Robert Téoule,⊥ and G. Victor Fazakerley*,‡

CEA, Service de Biochimie et de Génétique Moléculaire, Bât. 142, Département de Biologie Cellulaire et Moléculaire, CEA Saclay, 91191 Gif-sur-Yvette Cedex, France, Laboratoire de Physico-chimie Biomoléculaire et Cellulaire, CNRS URA 2056, Université Pierre et Marie Curie (T22), 4 Place Jussieu, 75252 Paris Cedex 05, France, Département de Recherche Fondamentale sur la Matière Condensée, Service de Chimie Inorganique et Biologique, Laboratoire Lésions des Acides Nucléiques, CEA Grenoble, 17 rue des Martyrs, F38054 Grenoble Cedex 9, France, and Département de Recherche Fondamentale sur la Matière Condensée, Service d'Etudes des Systèmes et Architecture Moléculaires, Laboratoire de Radiobiologie, CEA Grenoble, 17 rue des Martyrs, F38054 Grenoble Cedex 9, France

Received May 21, 1997; Revised Manuscript Received November 11, 1997

ABSTRACT: The presence of a *N*-(2-deoxy-D-*erythro* pentofuranosyl)urea (henceforth referred to as deoxyribosylurea) residue, ring fragmentation product of a thymine, in a frameshift situation in the sequence 5′d(AGGACCACG)·d(CGTGGurTCCT) has been studied by ^{1}H and ^{31}P nuclear magnetic resonance and molecular dynamics. At equilibrium, two species are found in slow exchange. We observe that the deoxyribosylurea residue can be either intra- or extrahelical within structures which otherwise do not deviate strongly from that of a B-DNA as observed by NMR. Our study suggests that this is determined by the nature and number of hydrogen bonds which this residue can form as a function of two possible isomers. There are two possible structures for the urea side chain, either cis or trans for the urido bond which significantly changes the hydrogen bonding geometry of the residue. In the intrahelical species, the cis isomer can form two good hydrogen bonds with the bases on the opposite strand in the intrahelical species, A4 and C5, which is not the case for the trans isomer. This results in a kink in the helical axis. For the major extrahelical species, the situation is reversed. The trans isomer is able to form two good hydrogen bonds, with G13 on the same strand and A7 on the opposite strand. For the extrahelical species, the cis isomer can form only one hydrogen bond. In this major structure the NMR data show that the bases which are on either side of the deoxyribosylurea residue in the sequence, G14 and T16, are stacked over each other in a way similar to a normal B-DNA structure. This requires the formation of a loop for the backbone between these two residues. This loop can belong to one of two families, right- or left-handed. In a previous study of an abasic frameshift [Cuniasse et al. (1989) *Biochemistry 28*, 2018−2026], a left-handed loop was observed, whereas in this study a right-handed loop is found for the first time in solution. The deoxyribosylurea residue lies in the minor groove and can form both an intra- and an interstrand hydrogen bond.

Ionizing radiations, produce free radicals in aqueous solution and can give rise to base modifications, single or double-strand breaks (Fuciarelli & Zimbrick, 1995; Cadet et al., 1997). Among the important base damaged products are the thymine ring fragmentation product residues such as deoxyribosylurea (Téoule et al., 1977). These are also produced by endogenous oxidation of DNA. Hydroxyl radicals are generated in aerobic cells by oxidative stress [for a review, see Cadenas (1989)]. The urea residues have lost part of their original coding information. They have been shown to strongly block DNA polymerase in vitro, the terminal site situated generally one base prior to the lesion (Evans et al., 1993). The fragmentation base products such as deoxyribosylurea are poorly bypassed by the DNA polymerase, even in the presence of SOS-induction. In certain sequence contexts, however, the urea lesion appears to be able to direct nucleotide incorporation. Urea sites appear to be as mutagenic as abasic sites derived from purines. Recent studies have indicated that urea residues preferentially promote misincorporation of guanine (Maccabee et al., 1994). However, the sequence context plays

† This work was, in part, financed by a grant from the Ministère de l'Education Nationale, de l'Enseignement Supérieur et de la Recherche, ACC-SV8.

* Author to whom correspondence should be addressed. Telephone: +(33) 1 69088087. Fax: +(33) 1 69084712. E-mail: victor@jonas.saclay.cea.fr.

‡ Service de Biochimie et de Génétique Moléculaire, CEA Saclay.

§ Université Pierre et Marie Curie.

|| Laboratoire Lésions des Acides Nucléiques, CEA Grenoble.

⊥ Laboratoire de Radiobiologie, CEA Grenoble.

[1] Abbreviations: NMR, nuclear magnetic resonance; NOE, nuclear Overhauser effect; NOESY, nuclear Overhauser effect spectroscopy; 1D, one dimensional; 2D, two dimensional; TOCSY, total correlation spectroscopy; MD, molecular dynamics; HSQC, heteronuclear single quantum correlation spectroscopy; Ur1 and Ur2, the duplexes containing, respectively, the major and the minor isomer of the *N*-(2-deoxy-D-*erythro*-pentafuranosyl)urea (referred to as deoxyribosylurea in the text) residue and ur^{i} and ur^{e}, the intrahelical and the extrahelical residue.

S0006-2960(97)01202-6 CCC: $15.00
Published on Web 01/06/1998

an important role in the base selectivity by the polymerase, and a thymine can be incorporated opposite the urea.

In a previous paper, we have reported a structural analysis by ^{1}H NMR[1] of deoxyribosylurea incorporated opposite either a thymine or a guanine in DNA (Gervais et al., 1992). We observed two species and presumed that these corresponded to the two isomers, cis and trans around the urido bond of the urea which were present in solution in the ratio 1:2.

Deoxyribosylurea residues could be considered as an intermediate structure between Watson−Crick bases and abasic sites. Part of the coding information has been lost, but they are still potentially able to form hydrogen bonds.

Many structures of DNA duplexes with bulges of one unpaired base have been reported because of their involvement in frameshift mutagenesis. In general, NMR studies have shown that purines stack inside the helix, producing a kink without major distortion of the backbone (Hare et al., 1986; Roy et al., 1987; Woodson & Crothers, 1988, 1989; Kalnik et al., 1989a; Nikonowicz et al., 1989, 1990; Rosen et al., 1992). However, it has been reported in a crystallographic study (Joshua-Tor et al., 1992) that an extra adenosine can be extrahelical, but this is a special case because the base is intercalated in an adjacent duplex in the lattice. On the other hand, bulged pyrimidines are generally extrahelical (van den Hoogen et al., 1988a,b; Kalnik et al., 1989b, 1990; Morden et al., 1990, 1993). This requires the formation of a loop conformation in order that the two bases adjacent to the extrahelical base are able to stack over each other. However, intrahelical structures for bulged pyrimidines have also been reported depending on the sequence context.

While structure determination for an intrahelical bulged species may be relatively straightforward in that the interresidue interactions are similar to those observed for B-DNA, the structure of extrahelical bulges cannot be predicted. We have previously reported studies on an extrahelical abasic frameshift sequence (Cuniasse et al., 1989; Cognet et al., 1990). In general, there are two ways of forming a simple backbone loop structure. Following the backbone it can either turn left-handed for the bulge (Cuniasse et al., 1989) or right-handed (Joshua-Tor et al., 1992) with a variety of subtle variations within these two families. The nature of the loop structure can be determined by unusual deoxyribose−deoxyribose NMR interactions (Cuniasse et al., 1989). Local dynamics can be very different, as we have observed for an extrahelical cytosine where even the CH6−H5 NOE was zero (Cuniasse et al., 1990).

A structure of an oligonucleotide containing an unpaired deoxyribosylurea is now investigated; this is formed during replication when the polymerase fails to incorporate a base opposite the urea site, giving rise to a frameshift structure. Multiple conformations and structures could exist or coexist for this DNA sequence. It has been reported that the urea side chain can exist in cis and trans conformations (Guy et al., 1990), but also that the deoxyribosylurea residue can be a mixture of α and β anomers (Baillet & Behr, 1995). We must also take into account that for all these structures the modified residue can be either intra- or extrahelical.

MATERIALS AND METHODS

The decamer containing the deoxyribosylurea residue was synthesized and purified as described previously (Guy et al., 1990; Gervais et al., 1992). The two strands corresponding to the different species of the deoxyribosylurea residue were then separated by reversed phase (Lichrosorb C18 column, 7 μm, 1 cm × 25 cm, Merck) high-performance liquid chromatography using a mobile phase of 5.7−6.3% acetonitrile in 0.1 M lithium chloride buffer (pH 6.5) over 40 min. The eluate volume was reduced to 3−4 mL, and the purified oligomers were precipitated with cold 1:1 ethanol:acetone solvent (20 mL), pelleted, washed with cold 70% ethanol, and lyophilized.

The sequence is

A1	G2	G3	A4		C5	C6	A7	C8	G9
T19	C18	C17	T16	ur15	G14	G13	T12	G11	C10

where A1−G9 is a continuous strand.

The duplexes were 2 mM in single strand concentration dissolved in 10 mM phosphate buffer, 150 mM NaCl, and 0.1 mM EDTA. Chemical shifts were measured relative to the internal reference tetramethylammonium chloride, 3.18 ppm. NMR spectra were recorded on either Bruker AMX500 or AMX600 spectrometers. NOESY spectra were recorded at different temperatures in the range 5−30 °C with mixing times of 45, 60, 80, 100, and 400 ms in D_2O and 250 ms in H_2O, in the phase-sensitive mode (Bodenhausen et al., 1984). The residual HDO resonance was presatured during the relaxation delay for spectra in D_2O. After zero-filling, the data were multiplied by a 5−15° shifted sine bell function in both dimensions. Distance determination from the initial NOE build up curves was done as described previously (Cuniasse et al., 1987). For the 1D and 2D spectra in H_2O, a jump- and return sequence was used to suppress the water signal (Plateau & Guéron, 1982). The pulse maximum was at 15 ppm. TOCSY experiments were recorded in the phase-sensitive mode (Davis & Bax, 1985) with MLEV-17 spin lock. DQF were recorded (Rance et al., 1984) with time-proportional phase incrementation. One dimensional ^{31}P spectra were recorded between 1 and 36 °C, and a 2D HSQC (Bodenhausen & Ruben, 1980) spectrum was recorded to allow resonance assignment.

Model Building and Molecular Dynamics. The charge distribution of the urea side chain was computed with the program QUEST (Singh & Kollman, 1984) for compatibility with the AMBER distribution force field (Weiner et al., 1986). All initial structures were generated from canonical B-DNA (Arnott et al., 1976), and all energy refinements and molecular dynamics (MD) were carried out with the program AMBER (Weiner et al., 1984) as in previous studies (Gervais et al., 1995; Boulard et al., 1995; Cognet et al., 1990, 1995) because the protocols used were found to reproduce most of the detailed behavior of an entire series of duplexes with different mismatches. In the present study, they were found to be very valuable to explore the conformational space from different starting structures. All MD runs were performed over 200 ps with restraints on all δ torsion angles to reinforce the observed C2′-*endo* conformations except for the deoxyribosylurea and T16 residues in the extrahelical species (see Results and Discussion). As in previous studies, MDI runs include NMR constraints and were used in the final stages of the molecular modeling. MDII runs were computed without distance constraints and were used to explore the

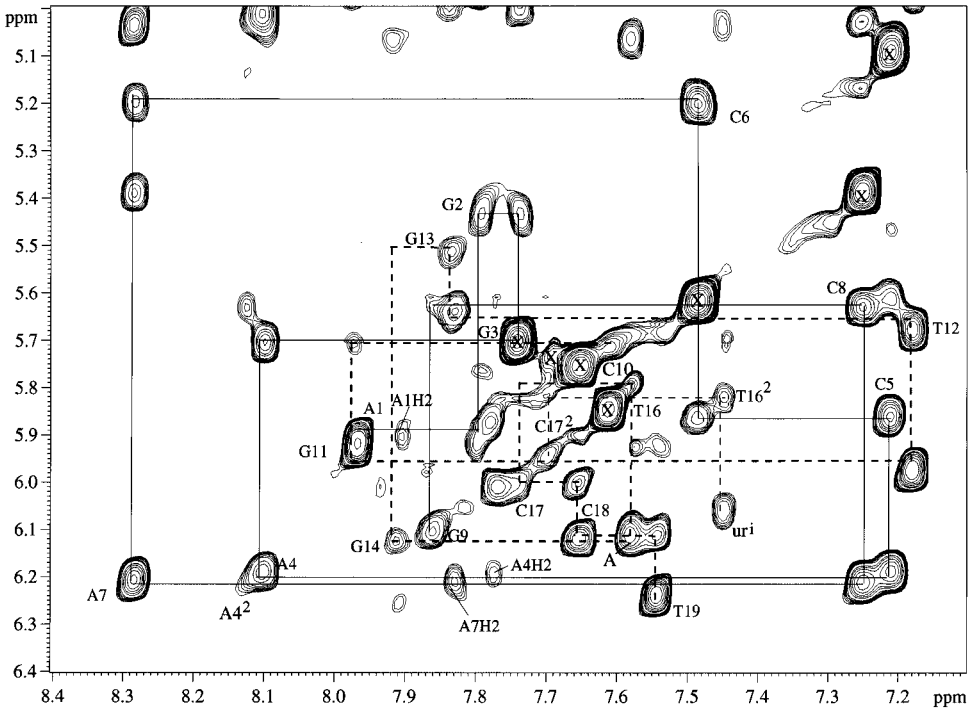

FIGURE 1: Expanded contour plot of the H6/H8−H1′/H5 region of the NOESY spectrum (400 ms mixing time) of the duplex at equilibrium at 27 °C in ^2H_2O, pH 6.1. Cross-peaks marked with an X correspond to H5−H6 interactions. Superscript 2 indicates residues for which separate resonances were observed for the Ur2 duplex. Peak A corresponds to the NOE between G16 and A14.

structural stability of different starting structures and/or the conformational space. All starting structures were systematically tried with the urea side chain in cis and trans forms for both the intra- and extrahelical forms.

RESULTS AND DISCUSSION

Spectra of the Major Species Ur1. A NOESY spectrum was recorded at pH 6.7, 30 °C, with a 400 ms mixing time on the duplex containing the major species Ur1 soon after annealing and cooling. At this time, the 1D spectrum in D_2O showed no signs of impurities or minor species (not shown).

For the first strand, we can follow the connectivities from G9 to A1 in both the H8/H6−H1′ and H8/H6−H2′/H2″ regions without interruption (see below). We note that the interactions for the central part of the strand are normal, suggesting that no major disruption of the helix takes place between C5 and A4, the residues which could be influenced by the deoxyribosylurea residue on the opposite strand.

For the second strand, we can follow the connectivities from T19 to T16 and from G14 to C10. Further, we observe direct interactions between T16H6 and G14H1′/H2′/H2″ and also between G14H8 and T16CH_3 which show that the G14 and T16 bases must be stacked over each other (see below).

Spectra of the Minor Species Ur2. We have also recorded spectra on the duplex containing the minor species of the deoxyribosylurea, Ur2. The 1D spectrum of the single strand showed, as for the major species, that it was greater than 95% pure. Titration of the Ur2 strand against strand 1 took 4 times longer than with the strand Ur1, as the resonances which could be integrated against each other (e.g., TH6 resonances) were not as well resolved. At the end of the titration, it became clear that another species had appeared in the spectrum. When we recorded a NOESY spectrum of the duplex with Ur2, we observed the presence of a second species. Comparing the sets of data for the two duplexes, we found that what was appearing in duplex Ur2 corresponded to the spectrum already recorded on the duplex Ur1.

Similarly, when we rerecorded data on the duplex Ur1 after several weeks, we observed a second species which corresponded to the initial Ur2 duplex. The two samples soon gave identical spectra with the two species, Ur2:Ur1, in a ratio of ca. 1:2. After this time, no further evolution was observed during several months. It is clear that we observed either an isomerization or anomerization process, not strand degradation which would have continued. As it is only possible to separate the two species at the single strand level, we decided to study the system at equilibrium as the duplex Ur1 had already been partly characterized.

Spectra of the System at Equilibrium. Nonexchangeable Protons. Figure 1 shows the H8/H6−H1′/H5 region of a NOESY spectrum recorded at 27 °C with a mixing time of 400 ms. Outside of the central part of the duplexes, A4−C6 and G14−C17, single resonances are observed for the protons of the two species. The chain of connectivities for the Ur1 duplex, which is the major species at equilibrium, can be easily followed. The C17H6−T16H1′ cross-peak and that of G14H8−G13H1′ are visible only at lower contour plot levels and are broad. We note that the T16H6−C17H5 cross-peak is also weak. The assignments are confirmed by analysis of the H8/H6−H2′/H2″/CH_3 region shown in Figure 2. We shall focus on the central part of the duplexes to investigate the nature of the two species. Figures 1 and 2 show the interactions described above between T16 and G14, peak A in Figure 1 and peaks B and C in Figure 2 confirming the stacking of T16 over G14. In neither of these two regions do we observe NOEs which could be assigned to the

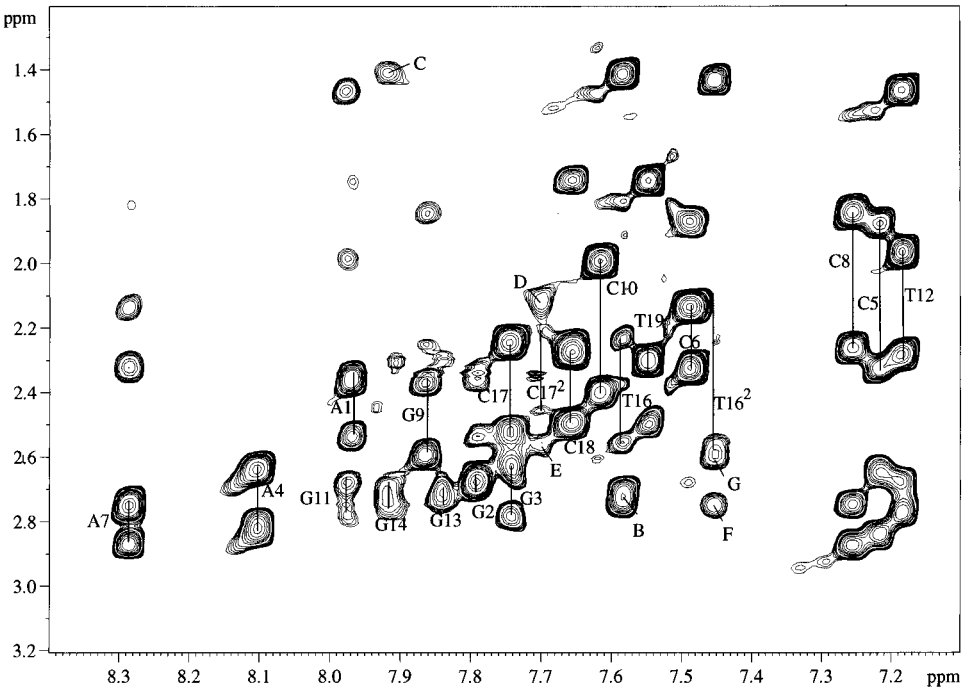

FIGURE 2: Expanded contour plot of the H6/H8−H2′/H2″/CH_3 region of the NOESY spectrum shown in Figure 1. The peaks marked B−G correspond to the following interactions: (B) T16H6−G14H2′/H2″, (C) G14H8−T16CH_3, (D and E) $C17^2$H6−$T16^2$H2′/H2″ , and (F and G) $T16^2$H6−ur^iH2′/H2″.

deoxyribosylurea residue with the aromatic protons of the Ur1 species.

The additional cross-peaks found in Figures 1 and 2 correspond to peaks observed in the first spectrum of the Ur2 duplex. In particular, the TCH_3 resonance at 1.42 ppm shows a cross-peak with an aromatic proton at 7.45 ppm. We do not observe a second interaction with the CH_3 group, which would be expected if there was a Watson−Crick base in the 5′ direction. We therefore assign the resonance at 7.45 ppm to the H6 proton of T16. Further, we observe an interaction between these two protons in a TOCSY spectrum (not shown), which confirms that they are of the same base. In this same spectrum, we observe an additional CH5−CH6 cross-peak at 5.73−7.69 ppm. We can follow the connectivities between the TH6 proton at 7.45 ppm and the CH6 proton at 7.69 in Figure 1, and this dinucleotide must correspond to $T16^2$ and $C17^2$ for the Ur2 duplex. This shows that the second $T16^2$H6−H1′ interaction observed at 6.06 ppm in Figure 1, for which no further sequential connectivity is observed, must be that of the H1′ of the deoxyribosylurea residue. This is confirmed in Figure 2 where the interactions $C17^2$−$T16^2$−ur, $C17^2$H6−$T16^2$H2′,H2″ (peaks D and E), and $T16^2$H6−urH2′,H2″ (peaks F and G) are identified. The second intraresidue cross-peak $T16^2$H6−H2′ is visible when the data are less severely filtered and is aligned with peak D. For this species the deoxyribosylurea residue must be intrahelical (ur^i), whereas for the major species it is extrahelical (ur^e).

From the NOESY and TOCSY spectra, the complete assignment of the sugar protons of the Watson−Crick bases and of the ur^i residue has been obtained. The region of the H3′−H4′ interactions of a TOCSY spectrum is shown in Figure 3. We observe, at 5.04/4.58 ppm, an extra cross-peak, which does not correspond to a deoxyribose of one of the Watson−Crick base pairs or of the intrahelical deoxyribosylurea residue. A resonance at 2.13 ppm shows a strong interaction with both of these protons which we assign to the coincident H2′/H2″ protons of the extrahelical deoxyribosylurea residue. We do not observe in the TOCSY or NOESY spectra a cross-peak between the protons at 2.13 ppm and a resonance at lower field than 5.04 ppm, which suggests that the latter is the H1′ proton of the extrahelical deoxyribosylurea residue.

We have recorded a series of NOESY spectra at short mixing times to measure the NOE build-up curves for determining proton−proton distances (see below). We have measured the intensity of the NOE between the H2′/H2″ protons at 2.13 ppm in the spectrum recorded with a 45 ms mixing time and the resonances at 5.04 and 4.58 ppm. If these two protons correspond to H3′ and H4′ protons, we would expect a difference of, at least, an order of magnitude between the two interactions. We observe that the NOE to the resonance at 4.58 ppm is 20% smaller than that for the resonance at 5.04 ppm. The only possible explanation is that the resonance at 5.04 ppm corresponds to the H1′ of the extrahelical deoxyribosylurea residue and that at 4.58 ppm to the H3′ proton. The H4′ and H5′/H5″ can now be identified. Having completed the resonance assignment of the two species, we need to know the origin of the changes observed in the spectra as a function of time.

Conformation of the Deoxyribosylurea Residue. It has been reported that deoxyribosylurea can exist in different forms. Cis and trans isomers can be formed for the pseudo peptide bond of the urea chain (Guy et al., 1990). More recently, it has been reported that this residue can also exist in an equilibrium between α and β anomers (Baillet & Behr, 1995). To differentiate between these two possibilities, we recorded DQF spectra to measure the sum of the H1′-H2′/H2″ coupling constants. We would expect that ΣH1′ would be unchanged or very little influenced between the two isomers, whereas it would be significantly smaller for the α anomer than for the β anomer. We observe that ΣH1′ is

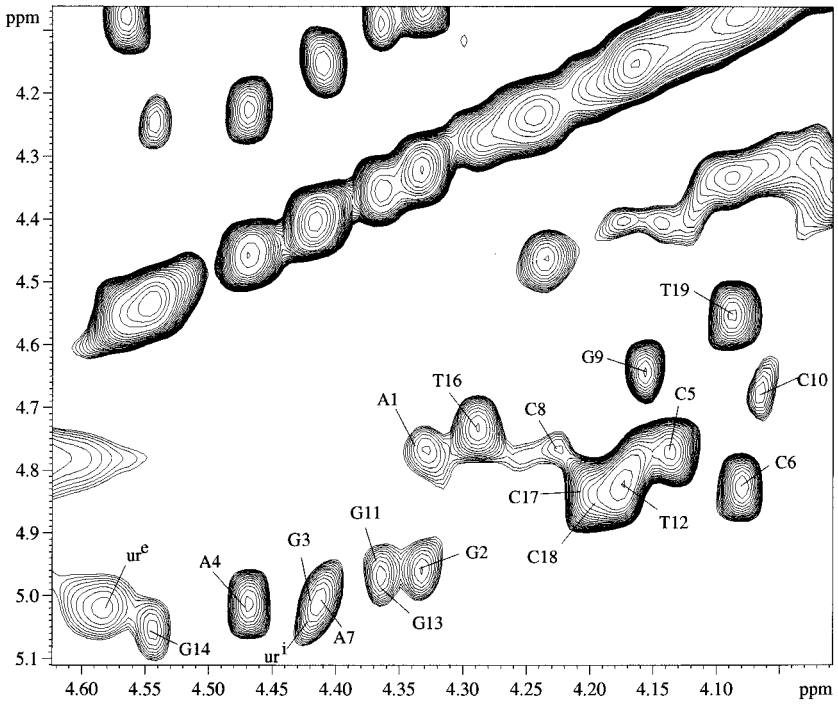

FIGURE 3: Part of the correlations H3′−H4′ of the TOCSY spectrum with an 80 ms mixing time.

14.6−14.8 Hz for both ur^e and ur^i, and we conclude that in the system we are observing here, there is a mixture of isomers rather than anomers.

Sugar Conformations. In the DQF spectra we were not able to measure all the necessary coupling constants to determine the sugar puckers because of resonance overlap. Those that could be measured indicated only C2′-*endo* puckers. The spectral dispersion was better in the H8/H6−H2′,H3′ regions. For NOESY spectra with short mixing times, the ratio of these two interactions gives a good measure of the sugar pucker (Cuniasse et al., 1989). Interestingly, only for the T16 of the duplex Ur1 do we observe a significant contribution from a C3′-*endo* conformation of ca. 50%. We were not able to determine the sugar pucker for the deoxyribosylurea in the extrahelical conformation, and in MD calculations described below no constraint was imposed.

At short mixing times, the NOEs observed between T16 and G14 for the duplex Ur1 correspond qualitatively to those observed between adjacent Watson−Crick base pairs, although their intensities were approximately half of those between normal base pairs. The base stacking must, however, have an orientation similar to that of a normal B-form DNA.

We have searched in all regions of the spectra for NOEs between the protons of ur^e and other residues. Those observed with T16, G14, and A7 and also those between T16 and G14 are summarized in Table 1. Although build-up curves have been measured, we do not want to overinterpret them as local dynamics may influence the data. Thus the NOEs are classed only in terms of their intensities. The interstrand $n + 3$ interactions for ur^e were unexpected but fit very well with the model proposed (see below). Build-up curves were measured for all the conformational sensitive proton−proton (on average 6−8 per residue) interactions, but only for the central part of the Ur1 strand did they show any significant deviation from those of classical B-DNA.

Table 1: Comparison of Distances Determined by NMR[a]

interaction (Å)	NMR	MD (Å)	stdev (Å)
intrahelical urea (ur^i)			
ur^i H5′−G14 H1′	s	2.9	0.40
ur^i H5′−G14 H2″	w	3.3	0.45
ur^i H1′−T16 H6	w	3.3	0.52
ur^i H1′−T16 CH_3	w	3.9	0.62
ur^i H1′−T16 H5′	w	3.5	0.74
ur^i H2′−T16 H6	w	3.6	0.92
ur^i H2′−T16 CH_3	m	3.6	0.71
ur^i H2″−T16 H6	s	2.8	0.56
ur^i H2″−T16 CH_3	m	2.8	0.27
ur^i H4′−T16 H5′	s	2.5	0.38
extrahelical urea (ur^e)			
ur^e H1′−A7 H1′	w	3.9	0.48
ur^e H1′−A7 H4′	s	2.8	0.52
ur^e H2″−A7 H4′	w	3.8	0.68
ur^e H2′−G14 H1′	s	2.8	0.36
ur^e H2′−G14 H4′	s	2.6	0.38
ur^e H5″−G14 H4′	m	4.1	0.32
ur^e H3′−T16 H6	m	4.3	0.46
T16 H6−G14 H1′	w	3.6	0.18
T16 H6−G14 H2″	m	3.6	0.60
T16 CH_3−G14 H8	w	4.2	0.22

[a] Interactions are classed as strong (s, <3.0 Å), medium (m, <3.6 Å), and weak (w, <4.5 Å), with the models proposed from MD I calculations for interactions observed with or within the central part of strand 2, T16-ur-G14. Where two protons are coincident, as for ur^e H2′/H2″, the distances given are for the shortest interaction.

Even the interactions in the central part of the opposite strand were normal. Similarly, the conformational changes for the Ur2 duplex were limited to the same residues, the data are given in Table 1.

Exchangeable Protons. One-dimensional spectra were recorded between pH 4.6 and 8 and at temperatures between 1 and 20 °C. Apart from line width changes, the spectra showed no significant changes. The best resolution was obtained at 5 °C and pH 6. Under these conditions we observe a resonance at 13.9 ppm which integrates for two protons, two thymines, and six resonances between 12.7 and

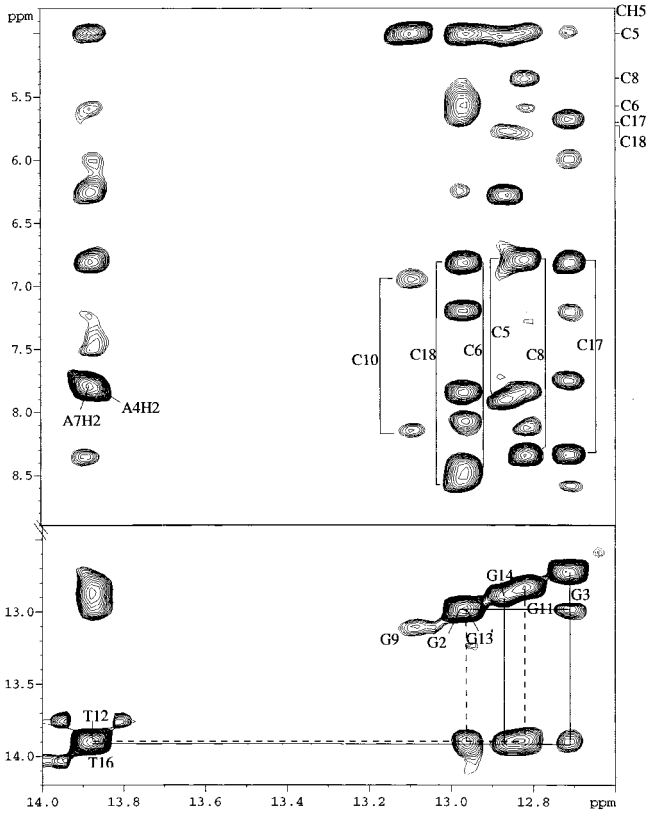

FIGURE 4: Part of the NOESY spectrum of the duplex in 90% H_2O recorded at 5 °C with a 250 ms mixing time. Region for imino−imino interactions (lower) and region for imino−amino, H2 interactions (upper).

13.1 ppm for the guanines. We were not able to find conditions where the thymine imino resonances were resolved, and the remaining thymine imino resonance, which is of a terminal base pair, most probably exchanges rapidly with the solvent.

Resonance assignment has been made from analysis of a NOESY spectrum recorded with a 250 ms mixing time. In the region of imino−imino interactions (Figure 4, lower), the connectivities G11−G13 are observed. The directionality is given as only G11 can show an NOE with the CH5 of C8 on the opposite strand. Similarly, the connectivities between G2 and T16 can be followed from both the imino−imino and imino−amino interactions. The last nonterminal G imino proton is assigned to G14 from its interaction with the A4H2 proton. This interaction, as well as the NOE observed between the imino protons of G14 and T16, shows the stacking of these two bases upon each other. We have not been able to observe separate imino resonances for the minor species, nor have we been able to find resonances for the NH protons of the urea chain. We would have expected that they are more protected from exchange with bulk solvent in the minor intrahelical form, but they must still remain accessible to bulk solvent.

^{31}P Spectra. The assignment of almost all of the resonances of the duplex has been obtained via analysis of a 2D ^{1}H/^{31}P heteronuclear single quantum correlation where we can follow the connectivities between the ^{31}P of the *i*th phosphate and both the H3′ (*i*) and H4′ (*i* + 1) (not shown).

We have been able to assign the ^{31}P phosphorus resonances for all the Watson−Crick bases outside the central trinucleotides. For the phosphates on either side of the ur^e and ur^i residues, we are able only to unambiguously assign one of them. This corresponds to the phosphorus of ur^e as we observe coupling with the adjacent residues, ur^{e}H3′and T16H4′. This resonance is shifted approximately 1 ppm downfield from the center of those corresponding to the Watson−Crick pairs. While this does not suggest a B_{II} conformation, which has been reported to give a resonance shifted by approximately 2 ppm (Chou et al., 1992), it does suggest that there is a modification of the backbone structure relative to classical B-DNA in the 3′ direction.

Determination of the Intra- and Extrahelical Structures. We observe two species in slow exchange on a proton NMR time scale. We cannot exclude that other minor species are present. We have shown that α anomers of the deoxyribosylurea are not major species. We observe without ambiguity an intrahelical species and also an extrahelical species. We have thus addressed the question as to whether the conformation is determined by the cis/trans nature of the pseudo peptide bond. The NMR data do not provide clear evidence to differentiate between the two isomers. We have therefore analyzed the possible hydrogen bonding structures for the two isomers, either intrahelical or extrahelical, and the necessary conformation of the deoxyribosylurea in order that either one hydrogen bond or two hydrogen bonds could be formed.

Intrahelical Stucture. The NMR data show that there is an intrahelical species from the NOEs observed between T16H6 and the deoxyribosylurea H1′, (Figure 1) and H2′/H2″ (Figure 2) and that the intrahelical deoxyribosyl moiety is positioned as in a normal B-DNA strand (Figure 5) and also that the sugar pucker is C2′-*endo*. These results clearly position in space the deoxyribosylurea residue which show the possibility for the formation of hydrogen bonds between the urea residue and the bases A4 and C5 on the opposite strand.

For the cis isomer, there is possible hydrogen bonding with either or both of these two bases. One of the protons of the urea side chain NH_2 can form a hydrogen bond with one of the possible acceptors, A4N1, C5O2, or C5N3. Also, the carbonyl group can be involved in a hydrogen bond with one of the amino protons of A4 or of C5. One such possibility is shown in Figure 6. As we have previously observed that in a model abasic site frameshift structure (Cuniasse et al., 1989) the deoxyribose was observed to be only extrahelical, it would appear necessary that one or more hydrogen bonds are involved in the stabilization of the intrahelical structure.

Three lines of arguments suggest that the cis isomer is intrahelical. Firstly, for the cis isomer it is possible to form good hydrogen bonds between ur^i(*cis*)O2···A4NH2 and/or ur^i(*cis*)NH2···C5O2 without deforming the structure from that of a B-DNA helix as shown in Figure 7. Secondly, because these hydrogen bonds are formed between the urea side chain and a base that is above or below on the opposite strand, the side chain must be orientated with a roll in either case. For both of these, the roll is in the same direction as for the adjacent bases and thus does not require further deformation of the helix. Another possibility is the formation of transient hydrogen bonds, ur^i*(cis)*O2−C5NH2 and ur^i-*(cis)*NH2−A4N1. However, for these, the roll has to be in the opposite sense to that of the adjacent base pairs and should be less favorable. Thirdly, although the urea side

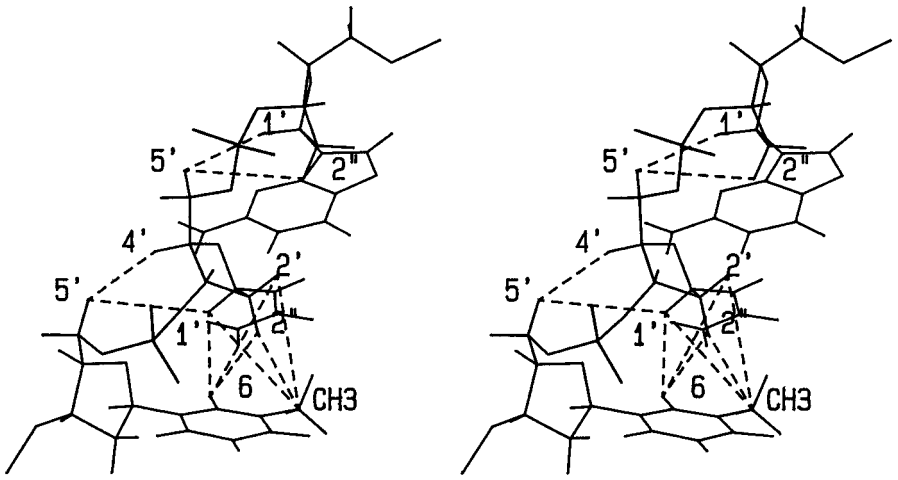

FIGURE 5: Detailed stereoview of the central part, G14 ur[i] T16, of the duplex. The dashed lines show the NOE interactions that are observed in the NMR spectra.

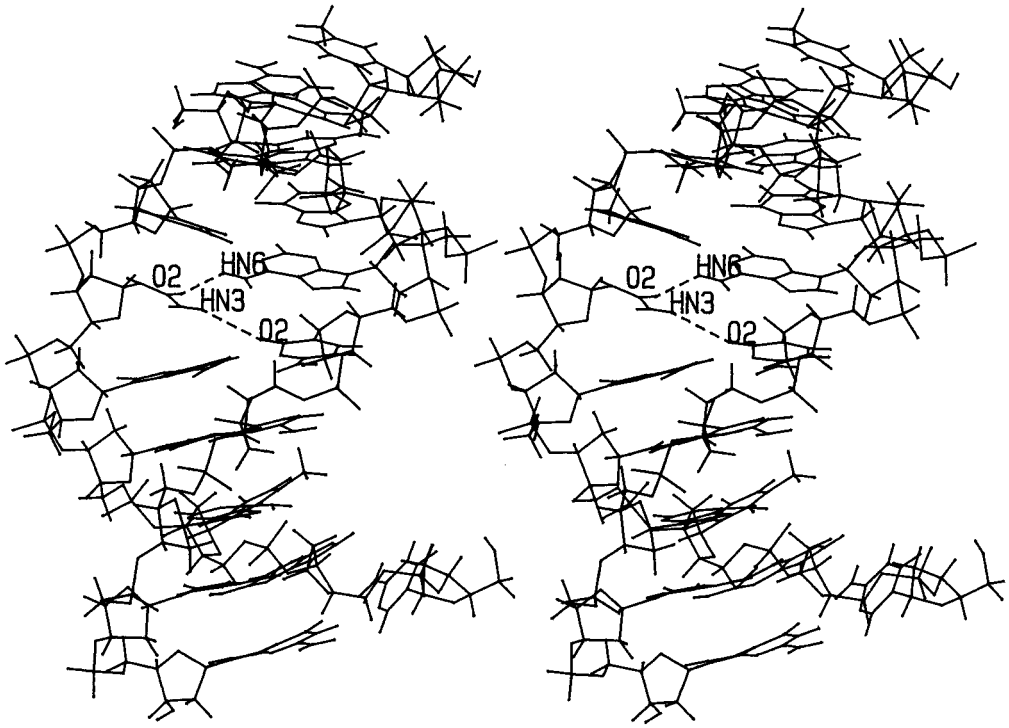

FIGURE 6: Stereoscopic view of the entire duplex showing the intrahelical cis deoxyribosylurea residue. This snapshot, observed from the minor groove during the molecular dynamics MDI runs, is characterized by two of the best hydrogen bonds that can be formed by the urea moiety: between a hydrogen of the amino group (HN3) of ur[i] and the O2 of C5 and between O2 of ur[i] and a hydrogen of the amino group of A4 (HN6). The orientation of the second strand, that contains the urea residue, is 5′ → 3′ from top to bottom.

chain could form simultaneously two hydrogen bonds with respectively only one base, either A4 or C5, in each case these hydrogen bonds must perturb the Watson−Crick geometry of either the base pair A4·T16 or C5.G14.

All of these structures were observed during the molecular dynamics runs, during which the δ torsion angles were all constrained to give C2′-*endo* sugar puckers, although hydrogen bonding ur[i](*cis*)O2···A4NH2 and/or ur[i](*cis*)NH2···C5O2 is most frequently seen. These hydrogen bonds require the least deviations from a B-DNA conformation in terms of backbone torsion angles, the least clashes concerning the roll and propeller twist with the adjacent bases and also they do not destabilize the adjacent base pairs. The torsion angles around ur[i](*cis*) are given in Table 2, and MD1 and MD11 calculations gave very similar results.

We have also analyzed the possible hydrogen bonding structures for the intrahelical trans isomer. This involves the same analysis as that for the cis isomer having exchanged, in space, the donor and acceptor of the urea moiety which drastically reduces hydrogen bonding possibilities unless there is a significant conformational displacement of the deoxyribosylurea residue which the NMR data do not indicate. Two hydrogen bonds cannot be formed simultaneously but single hydrogen bonding could occur between the ur[i]*(trans)*O2···A4 NH2 or C5 NH2 or between ur[i]*(trans)*NH2···A5 N1; however, in all cases the geometry is far from ideal. Although we have no direct evidence we conclude that the cis isomer is more likely to be intrahelical than the trans isomer.

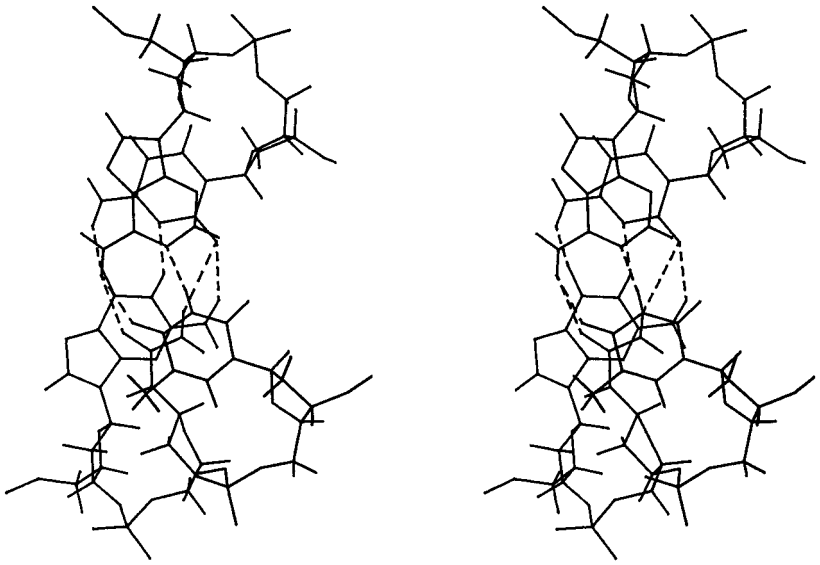

FIGURE 7: Stereoscopic view of the central part of the duplex, d(A4 C5)·d(G14 ur^{i} T16) seen from the 5′ end of the first strand. The urea residue, ur^{i}, is in the cis conformation and is inside the helix. This view shows the hydrogen bonds that may form between the urea side chain and the adenine A4 or the cytosine C5. These hydrogen bonds are represented by dashed lines.

Table 2: Average and Standard Deviations (in deg) for Torsion Angles Computed from MD Runs[a]

residue	pucker	stdev	amp	stdev	α	stdev	β	stdev	γ	stdev	δ	stdev	ϵ	stdev	ζ	stdev	χ
							Intrahelical Species										
av	139	15	43	5	−71	10	175	9	60	9	130	11	−178	9		12	−119
G 14	138	13	44	5	−69	10	178	9	59	9	130	10	−176	8	−98	13	−120
ur^{i}	135	16	44	5	−80	14	−173	10	50	9	128	12	−155	26		42	−95
T 16	146	18	40	6	−69	17	148	22	64	9	135	11	−163	33		43	−100
							Extrahelical Species										
G 14	135	15	43	6	−72	10	−177	9	53	8	131	10	−70	9	94	10	−98
ur^{e}15	133	27	38	6	140	28	−160	24	61	12	127	15	−106	17	−84	16	175
T 16	86	17	47	5	−72	11	177	12	57	10	86	12	179	8	−92	12	−142

[a] The line av corresponds to the average values observed for the Watson−Crick base pairs excluding the central trinucleotide and the terminal base pairs.

Extrahelical Structure. We have carried out the study for the trans isomer which could form hydrogen bonds in an extrahelical conformation. For the extrahelical species we observe that the Watson−Crick base pairs adopt a normal B-form DNA conformation with G14 and T16 stacked over each other as shown by the interproton interactions in Table 1. The sugars are all predominantly C2′-*endo* with the exception of T16 for which the NMR data show an equilibrium with a higher C3′-*endo* population. We are not able to determine the sugar pucker for the ur^{e} due to resonance overlap.

In a B-form DNA the adjacent phosphate groups are separated by ca. 7 Å, and when the sugar puckers are C3′-*endo* this distance is ca. 6 Å. In the case of an extrahelical deoxyribosylurea residue, the distance must be in this range in order to explain the observed NMR interactions between G14 and T16, whereas it would be 12−14 Å for the intrahelical species. In order to reduce the phosphate−phosphate distance, part of the sugar phosphate chain must form a loop such that G14 and T16 can stack over each other. Because of the relatively short length of this sugar phosphate chain and because of steric crowding, this segment cannot result from a combination of different types of loops and must remain simple. From a global and geometric point of view, formation of the loop can be approached along the sugar−phosphate backbone can be formed either by turning in a right-handed or left-handed direction. This is a first approach as this loop can subsequently be deformed to account for specific interactions between the bulged residue and residues belonging to the same or another helix. A left-handed looped- out structure has been observed for an abasic frameshift (Cuniasse et al., 1989; Cognet et al., 1990) and right-handed looped-out structures have been observed for an extrahelical adenosine in crystal structures (Joshua-Tor et al., 1992).

In the left-handed looped-out structure constructed from previous data (Cuniasse et al., 1989; Cognet et al., 1990), the plane associated with the sugar of the deoxyribosylurea residue would be tangential to the helical cylinder and the residue directed perpendicular to the helix axis on the major groove side. The urea side chain cannot interact with the rest of the helix and is completely exposed to the solvent. This type of loop is not constrained and would yield interproton distances between the deoxyriboses of ur^{e} and G14 that are not observed in the present study. For this reason, it must be excluded.

The right-handed looped-out structures which have been reported (Joshua-Tor et al., 1992), are a special case in that the extrahelical adenosine is intercalated between two bases of a parallel duplex in the crystal lattice. It cannot be used, as such, because the deoxyribose of the bulged adenine is directed along a radius of the DNA, perpendicular to the

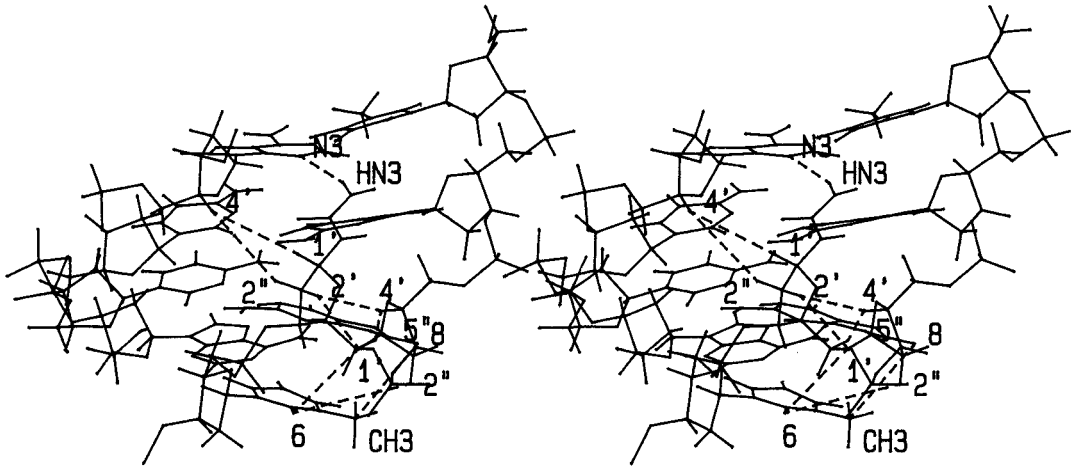

FIGURE 8: Stereoscopic view of the central part of the duplex, d(A4 C5 C6 A7)·d(T12 G13 G14 ur^e T16) showing the looped-out structure with the urea residue, ur^e, which lies in the minor groove, showing interactions through hydrogen bonding, between a hydrogen of the amino group (HN3) of the urea residue ur^e and the N3 of A7 and also between the oxygen O2 of the urea chain and the amino group of G13. This conformation is a representative snapshot of the average structure observed during molecular dynamics MDI. The dashed lines represent some of the interactions observed in the NMR spectra.

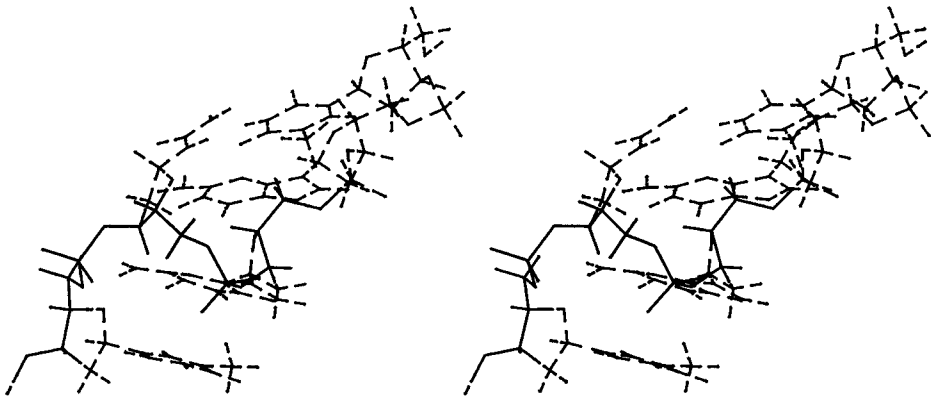

FIGURE 9: Detailed view of Figure 8 for the second strand T12 G13 G14 ur^e T16. The sugar−phosphate backbone of the central part is shown with solid lines, whereas the rest of the structure is plotted with dashed lines, to emphasize the loop structure of the backbone.

helix axis and oriented outward. For an isolated duplex, the hydrophobic adenine might not be totally exposed to the solvent as it would be in these structures. With this geometry, there would be no interaction between the ur^e deoxyribose and the rest of the helix. Depending on crystallization conditions, two different structures, where the loop appears to be constrained differently by the crystal structure, were found. In the absence of the spatial constraint on the extrahelical base, the right-handed loop may give rise to proton−proton interactions between the deoxyriboses of ur^e and of G14.

The position and orientation of the deoxyribose of the residue ur^e must satisfy the requirements derived from NMR observations, Table 1. Figures 8 and 9 show the final result that we obtained based upon the following observations and criteria.

The 5′ side of the plane of the ur^e deoxyribose must be parallel to and partly overlapping with the 3′ side of the plane of the G14 deoxyribose to account for the interactions ur^{e}H2′−G14H1′ and ur^{e}H5″−G14H4′. This position and orientation of the plane of the deoxyribose is confirmed by the interactions observed on the other side of the ur^e plane between the ur^e deoxyribose and the A7 deoxyribose, Figure 8 and Table 1.

All of these interactions serve to define the spatial position of the plane of the ur^e deoxyribose. But they also give the orientation of the deoxyribose in this plane. In order to account for the strong NOE interactions ur^{e}H1′−A7H4′, ur^{e}H2′−G14 H4′ and ur^{e}H2′−G14H1′, the axis which passes through the midpoint between C3′ and C4′ and the C1′ of the ur^e must point along an axis approximately parallel to the helix axis and in the 5′ direction of its strand.

The deoxyribosylurea is therefore well positioned and oriented relative to the B-DNA double helix. Since it is located halfway on the sugar phosphate chain segment that joins G14 and T16, this position can serve to define the midpoint of the loop as well as the C4′−C3′ vector. This is in agreement with a right-handed loop.

With this information and the fact that G14 is predominantly in a C2′-*endo* conformation whereas T16 is in an equilibrium C2′/C3′-*endo*, we have to search for the conformation of the short sugar phosphate segments G14 O3′−P−O5′−C5′ ur^e and of ur^e O3′−P−O5′−C5′T16. The conformation of these short segments must be in continuity with the rest of the helical strand.

Analysis of the structure with the bulged abasic site showed that the variations of only three torsion angles from classical B-DNA angles were sufficient to account for the left-handed loop (Cuniasse et al., 1989): ϵ on the 5′ side of the abasic site and γ and ζ of the deoxyribose of the abasic site. This is why we have modified, by molecular mechanics, the least number of torsion angles in these segments for the

Table 3: Models and Torsion Angle Ranges Explored in the Investigation of the Backbone Loop Structure of the Extrahelical Species[a]

	C4'	C3'	O3'	P	O5'	C5'	C4'	C3'	O3'	P	O5'	C5'	C4'	C3'
Torsion angles	δ	ε	ζ	α	β	γ	δ	ε	ζ	α	β	γ	δ	
B-DNA	t	t	g-	g-	t	g+	t	t	g-	g-	t	g+	t	
Models	t	g-,t	a	a	a	g+,g-	g+,t	g+,g-	a	g+,g-	a	g+,g-	g+,t	
Family 1	t	·	g+	g+	g-	·	·	g-	·	·	·	·	g+	
Family 2	t	g-	t	·	g+	g-	·	g+	g+	·	·	·	g+	
structure 1	t	g-	g+	g+	·	·	·	g-	·	·	·	·	g+	
structure 2	t	g-	g+/t	·	g+/t	g-	·	·	g+	t	g+	t	g+	

[a] The letter a indicates that all conformations were studied. In the initial families and final structures only torsion angles differing from B-DNA are indicated, a dot indicates no change.

ur^e from classical B-DNA values to one of the three main conformations (g−, g+, and t; the letter a, Table 3, means that all three possibilities were explored). The list of torsion angles and of conformations that were tried to yield a structure compatible with the shape of right-handed loops and with the constraints of position and orientation indicated above for the ur^e deoxyribose is shown in Table 3. Some of these torsion angles could not be modified to the trans conformation because they produce an extended chain that is incompatible with the stacking of G14 over T16. This analysis produced two sets of conformations (Families 1 and 2) with differences from classical B-DNA, these torsion angles are given in Table 3. We have explored the conformational space about these resulting structures in molecular dynamics MDI and MDII runs. All these MD runs result in two stable conformations, structures 1 and 2, Table 3.

The former is characterized by ϵ(g−), ζ(g+) of G14, and α(g+), ϵ(g−) of ur^e. The latter conformation is characterized by ϵ(g−), ζ(g+/t) of G14, γ(g−) of ur^e, and changes on α, β, and γ on T16. Although considerable fluctuations are observed during the MD runs, both types of structures fit well the NMR data given in Table 1. As they are closely related, we present the first structure that involves the least number of torsion angle changes relative to B-DNA. The structure of the loop is shown in Figure 9, and the essential torsion angles are given in Table 3. During these MD runs we observe that the sugar pucker of T16, for which no constraint has been applied, is in equilibrium between C2′-*endo* and C3′-*endo* in agreement with the NMR data. Also, we observe that the torsion angles ϵ, ζ, of ur^e differ significantly from classical B-DNA, which is reflected in the ^{31}P spectra.

Due to proton exchange with bulk solvent, we have not been able to observe the NH and NH_2 protons of the urea chain. However, the NOEs with the nonexchangeable protons of the deoxyribose strongly limit the volume in space that this chain can occupy, as shown in Figure 8. MD runs that are in agreement with the observed NOEs, Table 1, for the nonexchangeable protons indicate the formation of a hydrogen bond between a proton of the amino group of the chain and the A7N3 on the opposite strand. This stabilizes the interaction in the minor groove. Further, a second hydrogen bond can simultaneously form between the carbonyl group of the chain and the amino group of G13 on the same strand as the deoxyribosylurea. As the hydrogen bond donors and acceptors belong to three different moieties, A7, G13, and the urea side chain of ur^e, one of the two hydrogen bonds will always be stronger than the other. These results were obtained with the trans isomer. We have also examined the possible structures that the cis isomer could adopt when placed in the minor groove. With certain deformations of the structure, one or the other of the hydrogen bonds described above could be formed but it is not possible to form both simultaneously.

Conclusion. The study of the deoxyribosylurea in this sequence has resulted in many unexpected new findings. These concern, in particular, the conformation of the sugar−phosphate backbone and unusual hydrogen bonding possibilities.

We have previously shown that an abasic site frameshift (Cuniasse et al., 1989) results in an entirely extrahelical structure with a left-handed backbone loop and with the deoxyribose tangential to the helix axis. An intrahelical abasic site was not observed.

The structures observed in this study are very different. The slow formation of a mixture of the two species from a single purified species was a complicating factor for the interpretation of the NMR spectra. But as relatively well-separated resonances for the residues of the central part of the strand containing the deoxyribosylurea, the structures of the two systems could be determined at equilibrium.

Firstly, we have shown by NMR that the predominant species is extrahelical and the minor species intrahelical and that these two species correspond to two isomers of the deoxyribosylurea and not two anomers. For the intrahelical deoxyribosylurea, the molecular modeling suggests that this must result from hydrogen bonding inside the helix. We have not been able to observe these hydrogen bonds due to rapid proton exchange with bulk solvent. However, we have been able to clearly position the deoxyribose in space, which limits the position of the side chain for the intrahelical species. As we have previously shown (Cognet et al., 1995), hydrogen bonding is possible with a base above or below and on the opposite strand. These hydrogen bonds can stabilize the intrahelical species because stacking energy interactions with the urea side chain are probably weak. Hydrogen bonding is favorable for the cis isomer of the deoxyribosylurea, whereas it is less so for the trans isomer.

For the extrahelical species, the position of the deoxyribosylurea is well defined in space from the NOEs with the adjacent bases. These show for the first time that for a bulge structure in solution that the loop conformation is right-handed. By molecular modeling, this positions the deoxyribosylurea in the minor groove with the adjacent bases in the sequence stacked over each other. Hydrogen bond formation is favorable for the trans deoxyribosylurea rather than the cis form. We note that the possible formation of an intrastrand hydrogen bond with the base $n - 2$ could stop the progression of the DNA polymerase.

The mechanism of repair of deoxyribosylurea residues in *Escherichia coli* involves firstly their recognition which is by a DNA glycosylase, endonuclease III, or endonuclease VIII which initiate the base excision repair pathway. These enzymes cleave the *N*-glycosyl bond and then on one side of the abasic site, the phosphodiester backbone [for a review,

see Wallace (1994)]. Recognition efficiency is influenced by the surrounding sequence context. For the intrahelical deoxyribosylurea frameshift residue a similar mechanism might apply. The deoxyribosylurea is probably easily recognized as an error due to its mobility in the interior of the helix, certainly more so than for mispairs between Watson−Crick bases. We are not aware of structural studies on the repair of extrahelical frameshifts. However, it has been shown (Slupphaug et al., 1996) that the repair of uracil bases begins with trapping the modified base in an extrahelical conformation. In both conformations described here, the structures are not rigid and an equilibrium in which the deoxyribosylurea is intrahelical or lies in the minor groove with others where it is well exposed outside the helix is very probable.

ACKNOWLEDGMENT

We are most grateful to INSERM-SC5 for allowing us to compute the urido charge distributions and to Mr. R. Attias for help with the CCDB.

REFERENCES

Arnott, S., Smith, P. J. C., & Chandrasekaran, R. (1976) in *Atomic coordinates and molecular conformations for DNA-DNA, RNA-DNA and DNA-RNA helices* (Fasman, G. D., Ed.) Vol. 2, CRC Press, Cleveland, OH.

Baillet, S., & Behr, J-P. (1995) *Tetrahedron Lett. 36*, 8981−8984.

Bodenhausen, G., & Ruben, D. J. (1980) *Chem. Phys. Lett. 69*, 185−189.

Bodenhausen, G., Kogler, H., & Ernst, R. R. (1984) *J. Magn. Reson. 58*, 370−388.

Boulard, Y., Cognet, J. A. H., Gabarro-Arpa, J., Le Bret, M., Carbonnaux, C., & Fazakerley, G. V. (1995) *J. Mol. Biol. 246*, 194−208.

Cadenas, E. (1989) *Annu. Rev. Biochem. 58*, 79−110.

Cadet, J., Berger, M., Douk, T., & Ravarat, J-L. (1997) *Rev. Physiol. Biochem. Pharmacol. 131*, 1−87.

Chou, S.-H., Cheng, J.-W., Federoff, O. Y., Chuprina, V., & Reid, B. R. (1992) *J. Am. Chem. Soc. 114*, 3114−3115.

Cognet, J. A. H., Gabarro-Arpa, J., Cuniasse, P., Fazakerley, G. V., & Le Bret, M. (1990) *J. Biomol. Struct. Dyn. 7*, 1095−1115.

Cognet, J. A. H., Boulard, Y., & Fazakerley, G. V. (1995) *J. Mol. Biol. 246*, 209−226.

Cuniasse, P., Sowers, L. C., Eritja, R., Kaplan, B. E., Goodman, M. F., Cognet, J. A. H., Le Bret, M., Guschlbauer, W., & Fazakerley, G. V. (1987) *Nucleic Acids Res. 15*, 8003−8022.

Cuniasse, P., Sowers, L. C., Eritja, R., Kaplan, B. E., Goodman, M. F., Cognet, J. A. H., Le Bret, M., Guschlbauer, W., & Fazakerley, G. V. (1989) *Biochemistry 28*, 2018−2026.

Cuniasse, P., Fazakerley, G. V., Guschlbauer, W., Kaplan, B. E., &.Sowers, L. C. (1990) *J. Mol. Biol. 213*, 303−314.

Davis, D. G., & Bax, A. (1985) *J. Am. Chem. Soc. 107*, 2820−2821.

Evans, J., Maccabee, M., Hatahet, Z., Courcelle, J., Bockrath, R., Ide, H., & Wallace, S. S. (1993) *Mutat. Res. 299*, 147−156.

Fuciarelli, A. F., & Zimbrick, J. D., Eds. (1995) *Radiation Damage in DNA*, Battelle Press, Columbus, OH.

Gervais, V., Guy, A., Téoule, R., & Fazakerley, G. V. (1992) *Nucleic Acids Res. 20*, 6455−6460.

Gervais, V., Cognet, J. A. H., Le Bret, M., Sowers, L. C., & Fazakerley, G. V. (1995) *Eur. J. Biochem. 228*, 279−290.

Guy, A., Ahmad, S., & Téoule, R. (1990) *Tetrahedron Lett. 31*, 5745−5748.

Hare, D., Shapiro, L., & Patel, D. J. (1986) *Biochemistry 25*, 7456−7464.

Joshua-Tor, L., Frolow, F., Appella, E., Hope, H, Rabinovitch, D., & Sussman, J. L. (1992) *J. Mol. Biol. 225*, 397−431.

Kalnik, M. W., Norman, D. G., Swann, P. F., & Patel, D. J. (1989a) *J. Biol. Chem. 264*, 3702−3712.

Kalnik, M. W., Norman, D. G., Zagorski, M. G.,Swann, P. F., & Patel, D. J. (1989b) *Biochemistry 28*, 294−303.

Kalnik, M. W., Norman, D. G., Li, B. F., Swann, P. F., & Patel, D. J. (1990) *J. Biol. Chem. 265*, 636−647.

Maccabee, M., Evans, J. S., Glackin, M. P., Hatahet, Z., & Wallace, S. S. (1994) *J. Mol. Biol. 236*, 514−530.

Morden, K. M., & Maskos, K. (1993) *Biopolymers 33*, 27−36.

Morden, K. M., Gunn, B. M., & Maskos, K. (1990) *Biochemistry 29*, 8835−8845.

Nikonowicz, E. P., Roongta, V., Jones, C. R., & Gorenstein, D. G. (1989) *Biochemistry 28*, 8714−8725.

Nikonowicz, E. P., Meadows, R. P., & Gorenstein, D. G. (1990) *Biochemistry 29*, 4193−4204.

Plateau, P., & Guéron, M. (1982) *J. Am. Chem. Soc. 104*, 7310−7311.

Rance, M., Sorenson, O. W., Bodenhausen, G., Wagner, G., Ernst, R. R., & Wüthrich, K. (1984) *Biochem. Biophys. Res. Commun. 117*, 479−485.

Rosen, M. A., Live, D., & Patel, D. J. (1992) *Biochemistry 31*, 4004−4014.

Roy, S., Sklenar, V., Appella, E., & Cohen, J. S. (1987) *Biopolymers 26*, 2041−2052.

Singh, U. C., and Kollman, P. A. (1984) *J. Comput. Chem. 5*, 129−145.

Slupphaug, G., Mol, C. D., Kavli, B., Arvai, A. S., Krokan, H. E., & Tainer, J. A. (1996) *Nature 384*, 87−92.

Téoule, R., Bert, C., & Bonicel, A. (1977) *Radiat. Res. 72*, 190−200.

van den Hoogen, Y. T., van Beuzekom, A. A., de Vroom, E., van der Marel, G. A., van Boom, J. H., & Altona, C. (1988a) *Nucleic Acids Res. 16*, 5013−5030.

van den Hoogen, Y. T., van Beuzekom, A. A., van den Elst, H., van der Marel, G. A., van Boom, J. H., & Altona, C. (1988b) *Nucleic Acids Res. 16*, 2971−2986.

Wallace, S. S. (1994) *Int. J. Radiat. Biol.* 66, 579−589.

Weiner, S. J., Kollman, P. A., Case, D. A., Singh, U. C., Ghio, C., Alagona, G., Profeta, S., Jr., & Weiner, P. K. (1984) *J. Am. Chem. Soc. 106*, 765−784.

Weiner, S. J., Kollman, P. A., Nguyen, D. T., and Case, D. A. (1986) *J. Comput. Chem. 7*, 230−252.

Woodson, S. A., & Crothers, D. M. (1988) *Biochemistry 27*, 445−455.

Woodson, S. A., & Crothers, D. M. (1989) *Biopolymers 28*, 1149−1177.

BI971202J